Energy & Environmental Science

Accepted Manuscript

ROYAL SOCIETY OF CHEMISTRY

www.rsc.org/ees

Energy & Environmental Science RSCPublishing

Review

Lithium Sulfur Batteries, A Mechanistic Review

Cite this: DOI: 10.1039/xoxxoooooox

M. Wild,[a] L. O'Neill,[a] T. Zhang,[b] R. Purkayastha,[a] G. Minton,[a] M. Marinescu[b] and G. J. Offer[b]

Received 20th April 2015,
Accepted 21st April 2015

DOI: 10.1039/xoxxoooooox

www.rsc.org/

Lithium Sulfur (Li-S) batteries are one of the most promising next generation battery chemistries with potential to achieve 500-600 Wh/kg in the next few years. Yet understanding the underlying mechanisms of operation remains a major obstacle to their continued improvement. From a review of a range of analytical studies and physical models, it is clear that experimental understanding is well ahead of state-of-the-art models. Yet this understanding is still hindered by the limitations of available techniques and the implications of experiment and cell design on the mechanism. The mechanisms at the core of physical models for Li-S cells are overly simplistic compared to the latest thinking based upon experimental results, but creating more complicated models will be difficult, due to the lack of and inability to easily measure the necessary parameters. Despite this, there are significant opportunities to improve models with the latest experimentally derived mechanisms. Such models can inform materials research and lead to improved high fidelity models for controls and application engineers.

Introduction

Lithium Sulfur (Li-S) batteries offer the next step change in battery technology for a range of markets. Li-S batteries have the potential to reach practical energy densities of 500-600 Wh/Kg (cell level) in the next few years and, in the long term, the potential to be cheaper due to the use of lower cost active materials. Li-S offers significant improvement over Lithium Ion (Li-ion) battery chemistries that are reaching the practical limits of their performance around 140-240 Wh/Kg (cell level). Li-S batteries have the potential to reduce range anxiety for users of electric vehicles, to lead to significant weight reduction and improved safety for pedestrian applications and to lighter, more flexible solar storage options for marine, military and domestic application. The main drivers for those technologies to adopt Li-S energy storage solutions are the need to reduce environmental impact and maintain or improve user experience.

[a] OXIS Energy Ltd, E1 Culham Science Centre, Abingdon, Oxfordshire, OX14 3DB, UK. E-Mail: mark.wild@oxisenergy.com

[b] Department of Mechanical Engineering, Imperial College London, SW7 2AZ, UK. E-Mail: gregory.offer@imperial.ac.uk

The Li-S family of battery technologies today already achieves 160-350 Wh/Kg in production cells but is currently limited to niche low power applications requiring modest cycle life. For broader uptake, solutions are required to address the unique features of Li-S chemistry that stifles potential;

i) **Capacity fade** due to degradation (Figure 1) of cell components in the harsh environment of the Li-S cell containing organic electrolytes, lithium metal anodes and reactive intermediates [1–3].

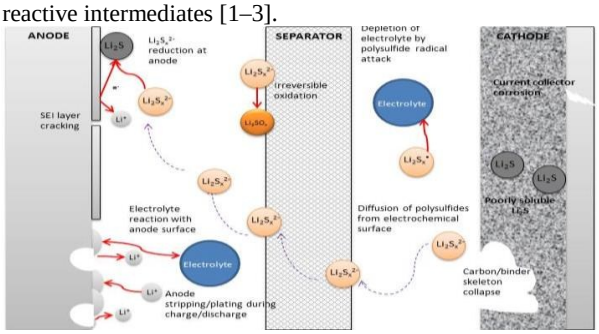

Figure 1 Summary of degradation mechanisms

Broader context

Next generation (beyond Li-Ion) battery systems such as Li-S are being developed to address the demand for safer, more energy dense batteries. This demand is driven by modern society, particularly decarbonising transport and enabling greater use of intermittent renewable energy sources. Next generation battery systems will also be a key enabling technology for a host of other applications such as off grid energy storage, aviation, autonomous robotics and mobile technology. In addition to better cells, designers of large and complex battery systems also require an improved understanding of these new battery technologies. Modelling provides a common interface between materials scientists and engineers, reducing the barrier to the acceptance of new technologies. Modelling has also been shown to accelerate technology development. Hence there is a need to both understand the mechanisms by which Li-S cells work and also how to model them. By supporting new high tech industries, next generation battery systems have the potential to offer huge economic benefits and improve lifestyles globally.

ii) **Shuttle phenomenon** where long-chain polysulfides diffuse to the anode and react to form shorter polysulfides that diffuse back to the cathode (Figure 2). This polysulfide shuttle corrodes the lithium anode and contributes to self-discharge and low coulombic efficiency [4–6].

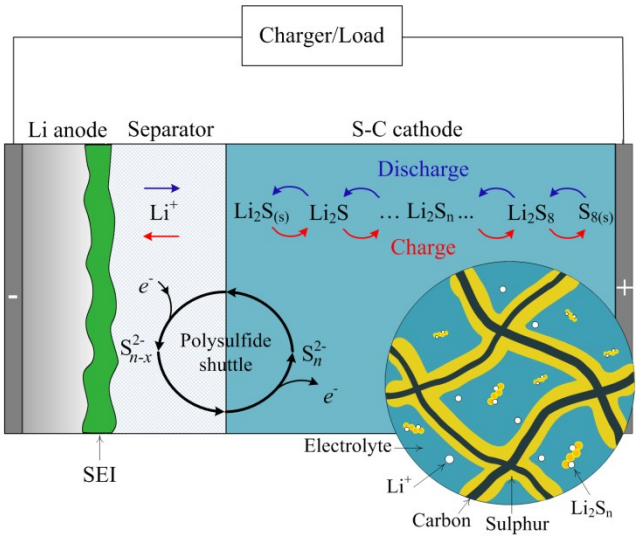

Figure 2 Summary of the effects of polysulfide dissolution, Shuttle phenomenon, effect on the cathode, insoluble products upon charge and discharge

iii) **Solubility of active species** leading to variable internal resistance and increased parasitic mass in cell construction from binders, conductive carbons and additives required to improve cathode conductivity. Both sulfur and its reduction product, lithium sulfide, are insulating and insoluble, resulting in chemical precipitation and dissolution towards the end of both charge (sulfur) and discharge (lithium sulfide) depending on voltage (Figure 2). During cycling this results in active material loss (both reversible and irreversible) in addition to cathode and separator deterioration, particularly the degradation of the porous structure [7–10].

iv) **Discharge/charge characteristics** such as the number of plateaus exhibited in the typical discharge curve, Figure 3, in contrast to a typical Li-ion curve. As a result, applications engineers require new tools to understand and work with Li-S batteries in applications.

Historically research has focussed on materials to address the challenges highlighted in (i-iii) and a number of recent publications are available summarising much of that effort [1, 53-60]. More recently, there have been efforts to better understand the discharge characteristics in detail, with a growing number of analytical studies on the polysulfide conversions taking place *in-situ* and *ex-situ*. Additionally, others have begun to model Li-S batteries in order to develop the tools required by applications engineers, and to help inform materials research [11].

The aim of this review is to bring together recent advances in the mechanistic understanding of Li-S batteries in order to facilitate the development of improved computational models of Li-S cells.

Experimental Techniques

A range of techniques have been used to probe the operating mechanisms of a Li-S cell, including electrochemical investigations and spectroscopic studies such as x-ray diffraction and liquid chromatography. Table 1 provides a summary.

Diffraction

X-ray diffraction (XRD) is used to study solid, crystalline materials and can give information regarding the crystal structure in the unit cell. As the majority of reactions in the Li-S cell occur in solution, S_8 and Li_2S are the only possible crystalline materials; therefore other species are not probed by this technique. XRD can give information on, for example, the extent of sulfur re-crystallisation during charge, or the state of charge, at which crystalline Li_2S begins to form during discharge, which can be indicative of the mechanistic pathways. XRD has been performed both *in situ* (during charge and discharge) and *ex situ* (on disassembled electrodes). *In-Situ* studies usually require synchrotron radiation in combination with a bespoke cell design, that allows for both the application and detection of the X-ray beam at different incident beam angles. Cells are cycled at low C rate, and XRD scans are then performed at pre-determined intervals, with a beam angle step time short enough to ensure that the structures do not change during the scan.

Several studies of Li-S cells have been performed using *in situ* XRD. Each uses slightly different experimental parameters, the main difference being the electrolyte. All studies agree that crystalline S_8 rapidly disappears during discharge in the first half of the upper plateau and that sulfur dissolves into the electrolyte before the cell voltage reaches 2.2V. Sulfur reappears on charge at the end of the high plateau although the exact state of charge (SOC) where this occurs varies slightly.

There is disagreement on the emergence of Li_2S during discharge. Nelson *et al*. [12] did not detect crystalline Li_2S at any point during C/8 cycles in a LiTFSI/DIOX/DME electrolyte system, although they suggest that Li_2S should be present at the end of discharge and likely occurs in amorphous form. Lowe *et al*. [13] and Canas *et al*. [14] both detected Li_2S only at the end of the low plateau (at >80% depth of discharge, DOD) with $LiClO_4$/TEGDME and $LiPF_6$/TEGDME as respective electrolyte systems. Contrary to previous studies, Walus *et al*. [15] detected crystalline Li_2S throughout the entire low plateau during discharge, which suggested that low order polysulfides and Li_2S were formed simultaneously, and that the reduction of other polysulfides does not necessarily occur successively. A summary of the region within which crystalline S_8 and Li_2S were detected during *in-situ* XRD cycling is shown in Figure 3.

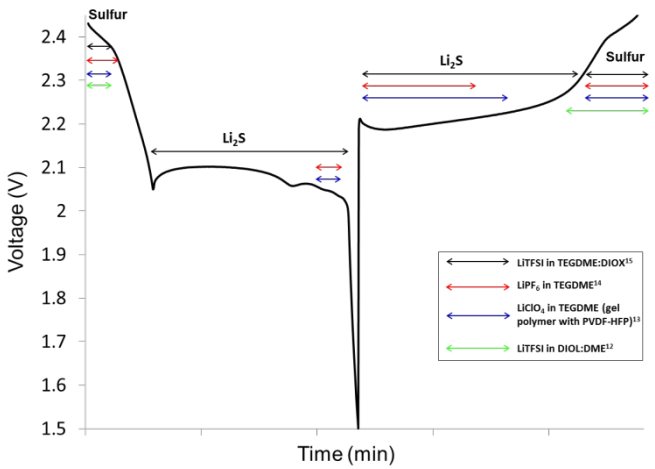

Figure 3 A comparison of S_8 and Li_2S detection by *in situ* XRD using different electrolyte systems.

Electrochemical

Electrochemical studies are the most common class of techniques used to characterise energy storage systems and involve the study of electron transfer. Electrochemical testing has been used extensively to study the effect of various cell component properties on performance. Several excellent reviews of these can be found elsewhere [16-20] and this review considers studies only concerning the mechanism of charge storage rather than general materials research.

Cyclic Voltammetry (CV) is typically configured with a three electrode cell design with all species in solution, and permits the potential and the number of electrons transferred in a redox reaction to be estimated. In Li-S cells however, it is difficult to obtain a stable reference electrode potential and so experiments are often performed with only two electrodes. The effect of solvent properties on the reduction of sulfur has been studied using CV with a three electrode cell and sulfur dissolved in various organic solvents [21]. The number and position of redox peaks varied according to the solvents ability to solvate the reduction products. When combining this data with theoretical calculations, it was concluded that the first reduction step (S_8 to S_8^{2-}) proceeded via 2 x 1 electron transfer rather than a 1 x 2 electron transfer. The solvents influence on sulfur redox potentials was confirmed by Gasteiger *et al.* [22], using cyclic voltammetry of glassy carbon electrodes in sulfur-containing electrolytes. When a DMSO-based solvent was used, an additional peak was seen at -1.2V vs Ag/AgCl when compared to DOL/DME based solvent. The additional peak was attributed to the choice of solvent changing the redox kinetics of the S_4^{2-} species, demonstrating the effect that the electrolyte formulation has on the mechanism of a Li-S cell.

Rotating ring disk electrode (RRDE) experiments are used to investigate the reaction kinetics of species formed at the electrode with reaction rates being calculated by varying the rotation speed. Lu *et al.* [22] used RRDE to determine the number of electrons transferred in each electrochemical step. Sulfur was supplied in dissolved form to provide 100% utilisation and three electrolyte systems were studied: high dielectric (DMSO), low dielectric (DOL/DME), and a lithium ion conducting solid electrolyte to prevent polysulfide shuttle/sulfur diffusion to the lithium anode. The numbers of electrons were calculated from Levich-Koutecky plots. The polysulfide diffusion coefficient was calculated by fitting the relation between the inverse of rotation speed and transient time in potential step experiments. They concluded that electrochemical steps only account for 25% of the total capacity i.e. four electrons per S_8 and, therefore, conversion of S_8 to Li_2S requires chemical polysulfide recombination and dissociation. Also, the solvation power of the solvent impacts the rate capability of the sulfur redox process. The rates of sulfur chain growth and disproportionation reactions are higher in low-dielectric solvents leading to higher rate capability.

Galvanostatic testing is the most commonly used technique for performance measurements, where the voltage response to a constant current is analysed. In a Li-S system, the potential of the various plateaus, as well as the ratio between the capacities of the two main plateaus and their decrease with cycling under certain experimental conditions, provides information about the mechanism taking place. A study by Schneider *et al.* [35] noted that the plateau potentials during charging and discharging varied when using different solvent systems. By measuring the lithium electrode potential in different solvents using a two chamber cell with a lithium electrode on each side, they concluded that the electrode potential depends not only on equilibrium constants, as defined by the Nernst equation, but also on some other property of the solvent. The differences in plateau potentials could not be explained by different species concentrations, such that the solvation energy of ions also contributes to the Gibbs energy of the system. Theoretical calculations of solvent complexation energies could explain the differences in the cell and plateau potentials. Highly polar or chelating solvents resulted in higher open circuit voltages (OCV's) and lower plateau potentials and, as the entire low plateau shifted, this suggests that Li_2S begins to precipitate at the start of the low plateau in agreement with Walus *et al.* [15]. However, when all species are in solution (i.e. at OCV), higher solvation energies lead to higher cell potentials. Once Li_2S begins to precipitate, removing species from solution, the cell potential reduces.

Electrochemical impedance spectroscopy (EIS) is used to monitor electrode reactions and transport properties over a wide range of frequencies, allowing reactions with different time constants to be separated in a non-destructive manner; however many times phenomena occur in the same location and at the same point in time. In order to understand the operation of the battery better, there is a need for analytical techniques to separate out these different processes, such as the development of symmetrical cells and impedance under load at different states of charge and discharge.

Experimental Techniques Benefits and Limitations

	Applications	Limitations
XRD [12-14]	Study formation of crystalline Sulfur and Lithium Sulfide during charge and discharge	Only S_8 and Li_2S visible; *Ex situ* results may be misleading as phase transitions may occur during rest or cell assembly; Cell designs for *in situ* analysis may not be representative of commercial cells.
CV and Galvanostatic testing [21-22]	Study electron transfer & redox reactions Discharge and charge curve analysis	Can only see electrochemical reactions, chemical reactions such as disproportionation of polysulfides are not observed; Quantitative analysis is difficult; Reactions that occur faster or slower than the testing time are not detected; When using fully dissolved species, the effect of cathode structure is not accounted for; Difficult to separate reactions occuring at the same potential.
RRDE [22]	Study reaction kinetics at the surface of an electrode	Can only see electrochemical reactions, chemical reactions such as disproportionation of polysulfides are not observed; Reactions that occur faster or slower than the testing time are not detected; When using fully dissolved species, the effect of cathode structure is not accounted for; Difficult to separate reactions occurring at the same potential Expensive and complex.
EIS [42-43]	Understand the resistance profile during cycling, providing information about interfaces and changes in the electrolyte	Can only see electrochemical reactions, chemical reactions such as disproportionation of polysulfides are not observed; Reactions that occur faster or slower than the testing time are not detected; When using fully dissolved species the effect of cathode structure is not accounted for; Difficult to separate processes occurring on the same timescales.
UV-Vis HPLC HPLC/ESI-MS [24-26]	Study polysulfides in solution with wavelengths and masses corresponding to chain length, and the characteristic response of the S_3 radical anion	Experimentally impossible to isolate individual polysulfides due to the propensity towards disproportionation and chain growth/ shortening. This makes interpretation of results difficult, as peaks fall within the same broad wavelength range; Bespoke cell designs are required for *in situ* studies as the light must pass through the sample for reflection. Holes in the lithium anode can lead to gradients of polysulfides and affects diffusion. For transmission, a larger distance between electrodes is requiring more electrolyte which affects solubility and species concentration; Polysulfide species are sensitive to air and moisture, requiring an inert experimental atmosphere; HPLC can not detect Li_2S, ESI-MS on unprotected polysulfides resulted in the formation of clusters. The method assumes that polysulfides do not interconvert during the derivatisation process.
NMR MS [27]	*Ex situ* analysis of the relative concentrations of polysulfide species	Often performed ex-situ and therefore may not be representative of *in operando* operation; ^{7}Li MAS spectra only show a clear peak for Li_2S and S_8, all other signals are a mixture of peaks requiring deconvolution; ^{33}S NMR signal is not strong enough for accurate interpretation; Derivatisation to trap polysulfides for *ex-situ* analysis by NMR or Mass spectrometry may alter the relative ratios of polysulfides.
XANES [28-29]	Study of electrolyte systems, polysulfides and cathode with encapsulated sulfur	XANES requires synchrotron radiation and bespoke cell design to allow X-rays to reach the relevant area of the cell being studied; Not all polysulfide species have been identified using XANES, for example S_5; Reference spectra often contain mixtures of species making the accurate assignment of peaks difficult.
ESR/EPR [50]	Study radicals in detail, S_3 radical anion is thought to be a key intermediate	Only looks at radical species.

Table 1 Summary of analytical techniques used in the elucidation of the mechanism of a Li-S cell

Macdonald and Johnson [44] divide the properties obtainable from impedance spectroscopy into two categories: 1. material properties such as diffusivity, mobility's, etc. and 2. interface properties such as capacitance of the interface region and adsorption-reaction rate constants. After obtaining the impedance response the system can be described in terms of equivalent circuit components, from which various resistance, capacitance and inductance values can be estimated to quantify the contribution of different physical and chemical processes to the overall impedance of the battery. The problem lies with interpretation of the results; the equivalent circuit is a 'lumped' response of the system. It is therefore not only possible to obtain the same response with a different combination of circuit elements, but to not accurately represent the spatial distribution of these electrochemical processes; instead the processes are averaged or smeared out. Hence, it becomes critical to have a working knowledge of the different processes that occur in the cell, and their relative contribution, in order to start with a sensible equivalent circuit.

Most of the proposed equivalent circuit models for Li-S are composed of few (two/three/even four) Randles circuits (R/C) connected in series. However, the interpretation of the physical meaning of each R/C is more complicated, and several discrepancies between interpretations exist [42, 43 & 45]. While there is a wealth of information that can be drawn from the system, the interpretation of the data is subjective in nature simply due to the large number of processes that occur concurrently within the cell. For the case of capacity fade and degradation, it is the relative change in the values of impedance that are important, as they indicate which components of the battery are changing.

Spectroscopic

Several spectroscopic techniques have been used to identify species within the Li-S system. Lithium polysulfides strongly absorb light in the UV-visible region. UV-Visible spectroscopy (UV-Vis) is used in particular for the S_3 radical anion, which appears blue in solution and gives a characteristic absorption band at 617nm [26]. Interactions between polysulfides and UV-Vis radiation depend on polysulfide chain length, alkali cation, the nature of the solvent, and the stability of the polysulfide species in the solvent. As a result, comparison of results should carefully consider the experimental reaction parameters.

Studies have been performed both *in situ* and *ex situ*. The characteristic spectra of individual polysulfides have been estimated by taking a UV-Vis spectrum of stoichiometric mixtures of lithium and sulfur in the electrolyte being studied. As the chain length decreases, the colour of the solution changes from red to green [24, 25] although peak assignment varies between studies and, to further complicate interpretation, is also dependent on the solvent. Patel *et al*. [24] used the first derivative of the UV-Vis spectra to more accurately assign peaks to specific polysulfide species. Their *in operando* experimental data supported the theory of polysulfide chain shortening during discharge and lengthening during charge. The data indicated specifically, that mostly Li_2S_8 and Li_2S_6 were present in the high plateau, Li_2S_4 and Li_2S_3 in the low plateau and Li_2S_2 and Li_2S at the end of the low plateau. The S_3 radical anion was unexpectedly not discussed, even though the electrolyte (LiTFSI/Sulfolane) has a relatively high dielectric constant and would be expected to stabilise radicals [22]. In contrast, an ex situ UV-Vis study by Cañas *et al*. [25] detected the S_3 radical anion from 25% DOD until 100% DOD, reaching a maximum concentration at 37.5%, despite employing a much lower sulfur content cathode (50% cf. 90%) and the low dielectric electrolyte system LiPF6/TEGDME. A similar study by Alloin and Barchasz [26], with a 50% sulfur content cathode and LiTFSI/TEGDME/DIOX electrolyte system, also detected the S_3 radical anion between 2.3 and 2.1V. Polysulfides were also methylated using methyl trifluoromethane sulfonate to stabilise them for analysis by HPLC, and it was found that polysulfide retention time increased with chain length. At 3V, S_8, S_8^{2-} and S_4^{2-} were detected. At 1.95V during reaction, S_2^{2-}, S_3^{2-}, S_4^{2-}, S_5^{2-} were detected and, after reaction (at 1.95 and 1.5V), no polysulfide species were detected suggesting complete conversion to Li_2S/Li_2S_2. Kawase *et al*. [27] calculated that the absorption bands for Li_2S_7, Li_2S_5 and Li_2S_3 overlap making them extremely difficult to determine using conventional UV-Vis techniques.

^{33}S Nuclear magnetic resonance (NMR) is not sensitive enough to elucidate different polysulfide structures, as individual polysulfide species are unstable and short-lived. Lithium polysulfide species have been stabilised by derivatisation with protecting groups such as benzylated polysulfides and identified by LC-MS [27]. In the benzylated state, the polysulfides were able to be analysed by proton NMR and liquid chromatography. When using a 60:30:10 sulfur: Carbon black: PTFE cathode and LiTFSI/DOL/DME electrolyte system, it was concluded that the dominant polysulfide species during the low plateau was Li_2S_3. Li_2S was detected at almost every stage during charge and discharge, even in the high plateau. The experiment involved stopping the charge/discharge test, de-constructing the cell, pulverising the cathode in a mixture of DME and benzyl chloride by ultra-sonication and waiting for up to 4 days. The results assume no inter-conversion of polysulfide species occurs during this process.

Earlier Diao *et al*. [52] had monitored polysulfide species at various states of charge using LC-MS without derivatisation. They found that even with electrospray mass spectrometry to reduce fragmentation of the polysulfides, the dominant species were polysulfide clusters (S_{18} to S_6) making interpretation difficult. Using a combination of ICP-OES to determine total sulfur content in the electrolyte and LC-MS to speciate the sulfur content the authors were able to draw some interesting conclusions. Total sulfur content in the electrolyte peaked in the high plateau (>2.2V) rather than at the dip suggesting a non-linear mechanism. The total sulfur content in the electrolyte reduced throughout the low plateau corresponding to the precipitation of Li_2S at the start of the low plateau. At the end of discharge 20% sulfur remained in the electrolyte, at the end of charge 45% when cycling between 1.7 and 2.4V. This ratio did not vary significantly with cycle life despite capacity fade, thus the equilibrium concentration of sulfur in the electrolyte has little impact on capacity fade.

XANES involves the absorption of X-rays by matter (compared with XRD where X-rays are diffracted with no change of energy). XANES has been used to study both the electrolyte system [28] and the cathode with encapsulated sulfur and polysulfides [29]. A study of the X-ray absorption spectra (XAS) of different solvents during cycling [28] could only identify S_8 and Li_2S species. It concluded that the discharge products of sulfur in DOL/DME and TEGDME were similar, suggesting that the reduction mechanism was similar in ether based solvents. Higher levels of self-discharge were seen in DOL/DME than TEGDME. A more comprehensive study by Cuisinier *et al.* first identified reference spectra of S_6^{2-} and S_4^{2-} by NMR spectroscopy, as well as S_8 and Li_2S, leading to a more complete picture of the reaction intermediates. Only one solvent system was studied-LiTFSI/DOL/DME with 2% $LiNO_3$ additive. They concluded that the gradual decline of Li_2S during charge was largely due to the formation of S_6^{2-}, but the continued presence of S_6 in the high plateau also suggests that S_8^{2-} is unstable and rapidly disproportionates. They mapped the relative contributions from each polysulfide species during charge and discharge, showing S_8 rapidly forming a stable equilibrium of S_6^{2-}, S_4^{2-} and S_8 in the high plateau. The concentration of each of these species remained fairly constant through much of the low plateau, until the onset of Li_2S formation at approximately 60% DOD. From this point the Li_2S concentration increased at the expense of higher order species, with the Li_2S hitting a maximum at 100% DOD.

During charge, the mechanism appears different and there is a less stable region of polysulfide species concentration. Li_2S is seen to reduce linearly across the charge cycle, whilst middle-order polysulfides reach some intermediate maximum concentration at about 50% SOC, before a large rise in S_8 towards 100% SOC. Thus the forward and reverse mechanism of a Li-S cell is not the same, which can be seen in the differing resistance profiles, Figure 4.

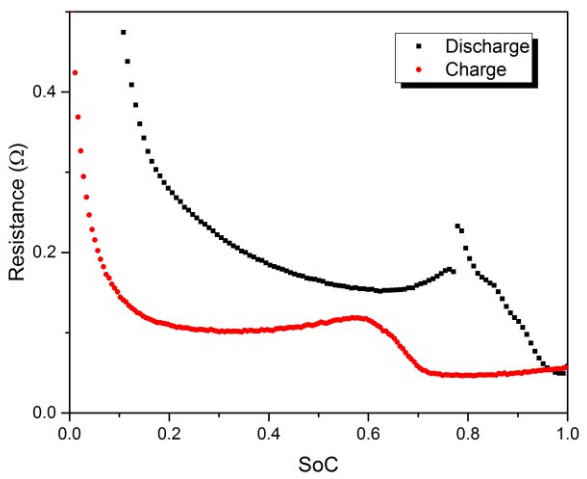

Figure 4 Resistance asymmetry between charge and discharge

More recently, Nazar *et al*. [30] identified the S_3 radical anion using XAS and demonstrated its role as a redox mediator in a Li-S cell stabilised by electron pair donor solvents (EPD). The S_3 radical anion was shown to contribute to *Ca.* 25% of the available polysulfides in EPD solvents and <<5% in glymes (such as DOL/DME). The number of solvating oxygen's also improved radical stabilisation, with TEGDME electrolytes appearing green (a combination of ultramarine blue from the S_3 radical and yellow from the presence of sulfur dianions). As EPD solvents also partially dissolve Li_2S, high sulfur utilisation was achieved initially with 98% of S_8 being converted from the cathode into stable intermediates in solution. Instability of EPD solvents with the lithium anode causes rapid degradation and currently precludes their application. The S_3 radical anion formed immediately reaches a maximum at *Ca.* 2.2V and then reduces until the end of discharge. Upon charge it is present throughout, except for in the fully charged state. The S_4 dianion was also monitored and found to increase throughout the discharge reaching a maximum at *Ca.* 1000 mAh/g sulfur.

Similarly Gorlin *et al.* [47] used K edge XANES to study intermediates in high (DMAC) and low dielectric (DOL/DME) solvents using a new *operando* cell design with good chemistry performance. Li_2S was observed after discharge of 4-5 e^-/S_8 in both electrolytes, however subsequent conversion of polysulfides to Li_2S was found to be more rapid in the low dielectric solvent. At the end of discharge, by subtracting the spectra for Li_2S, in the high dielectric solvent, Li_2S was detected in the presence of other polysulfide species. In the low dielectric, Li_2S was detected in the presence of a component that did not correspond to a typical polysulfide spectrum hypothesised to correspond to Li_2S_2/S_2^{2-}. S_8 was not detected at the end of discharge. It was concluded that disproportionation was faster in poorly rather than a strongly ion solvating environment, explaining the higher rate capability seen with low dielectric electrolyte systems such as those based on DOL/DME. Also, the different end products suggest that different mechanisms may contribute to reaching the end of discharge in two different ion-solvating environments. It was conjectured that in strongly ion-solvating environments the end point is reached after discharge of 12/16 e^-/S_8; as the lower order polysulfides are depleted they become more stabilised in the reduced form and do not readily disproportionate, leading to an increased overpotential necessary to maintain the current, and the subsequent end, of discharge. In poorly ion solvating environments, the stability of lower order polysulfides is less influential and an alternative species is stabilised that cannot disproportionate to be electrochemically reduced such as that proposed. The rate of precipitation may also be a factor blocking the electrochemically active surfaces.

Electron paramagnetic resonance (EPR) has recently been used to look more closely at the role of the S_3 radical anion. Wang *et al*. [31] have monitored its presence throughout both charge and discharge and have proposed that at 2.1V, a temporary, equilibrium exists between S_8, S_8^{2-}, S_6^{2-}, and the S_3 radical anion, while at the end of discharge, a similar equilibrium exists between S_6^{2-}, S_4^{2-}, Li_2S_3 (Major), Li_2S (Major) and again, the S_3 radical anion. This may explain an important phenomenon previously noticed; cathodes composed of Li_2S do not perform well and require a large over potential in contrast to cycled cells starting from sulfur. It is proposed that Li_2S is formed via two mechanisms, 1) electrochemically, controlled by current density and voltage cut off

and 2) chemically controlled by precipitation through the choice of electrolyte and, as such, trapping some of the radical anion in equilibrium. Upon charge, the presence of this potentially catalytic redox mediator may, in fact, lead to the direct formation of Li_2S and Li_2S_2 to Li_2S_4 and directly to Li_2S_8, where more of the S_3 radical anion can be generated through disproportionation. This implies the charge mechanism proceeds via a more direct pathway made more facile by the phase change from solid to liquid and the exposure of the electrode surface. In fact, surface catalysis may also play a role in heterogeneous chemical reactions of polysulfides but, thus far, this has not been reported in the literature.

Wu *et al.* [46] recently used *in-situ* Raman spectroscopy and cyclic voltammetry to investigate the potential dependence and rates of formation for sulfur species. The potential was switched between 3.2 and 2.2V using a LITFSI/TEGDME/DIOX electrolyte system. At 2.2V S_4^{2-}, S_4^-, S_3 radical anion, S_x^{2-} and $S_2O_4^{2-}$ were observed, and the intensity of peaks associated with short chain polysulfides grows at 2.2V with time. A pseudo first order fit was used to model the reaction kinetics. The S_3 radical anion appears with a rate constant equal to 0.091 +/-0.12 min^{-1}; the disappearance of S_8 had a rate constant of 0.103 +/- 0.023 min^{-1} suggesting that the short chain polysulfides are formed directly from S_8 dissociation. The rate constant for the formation of other short chain polysulfides also correlated, suggesting that there was no dominant short chain species formed directly from S_8. Upon charge the rate constant for the decomposition of the S_3 radical anion was 0.080 +/-0.018 min^{-1} and for the formation of S_8 0.114 +/- 0.029 min^{-1}, suggesting that the forward and reverse rate constants are similar and quasi reversible. Over the full discharge switching between 3.2 and 1.5V, S_8 disappears with a rate constant of 0.259 +/- 0.05 min^{-1} and the S_3 radical anion appears with a rate constant of 0.273 +/-0.041 min^{-1} during discharge. The 2-3 fold increase in rate constant is thought to be due to the greater driving force when switching from 3.2V to 1.5V than from 3.2V to 2.2V; again forward and reverse rate constants were similar. This approach, however, does not take into account the possibility of alternative pathways during charge and discharge as indicated by Gorlin *et al*. [47].

Li-S Mechanisms used in modelling

Mikhaylik and Akridge [32] developed a zero dimensional, thermally coupled Li-S battery model to study the effect of the polysulfide shuttle on charge/discharge voltage curves and the associated self-heating effect. The model computes the equilibrium potentials based on the Nernst equation for a simplified two-stage reduction scheme:

$$S_8 + 4e^- \rightarrow 2S_4^{2-} \quad \text{(419 mAh/g, High Plateau)}$$

$$S_4^{2-} + 4e^- \rightarrow 2S^{2-} + S_2^{2-} \quad \text{(837 mAh/g, Low plateau)}$$

Effects of kinetic over potential, electrolyte resistance, and dissolution/precipitation of polysulfides are not considered. The standard potentials for the two reactions are read from an experimental low-current discharge curve (C/30), to correspond to the particular species concentration ratios that yield $E=E_0$ in the Nernst equation. From this procedure the high plateau and the low plateau standard potentials are 2.33V and 2.18V respectively.

Moy *et al.* [39] derived a similar analytical model to study the polysulfide shuttle by adding intermediate sequential steps in the reduction chain and validated with experiment:

$S_8 + 2e^- + 2Li^+ \leftrightarrow Li_2S_8$	>2.3V
$3Li_2S_8 + 2e^- + 2Li^+ \leftrightarrow 4Li_2S_6$	>2.3V
$2Li_2S_6 + 2e^- + 2Li^+ \leftrightarrow 3Li_2S_4$	2.3 to 2.1V
$Li_2S_4 + 2e^- + 2Li^+ \leftrightarrow 2Li_2S_2$	1.9 to 2.1V
$Li_2S_4 + 6e^- + 6Li^+ \leftrightarrow 4Li_2S$	1.9 to 2.1V
$Li_2S_2 + 2e^- + 2Li^+ \leftrightarrow 2Li_2S$	<1.9V

In addition to the above electrochemical processes, they suggested the presence of a chemical disproportionation reactions to explain negative shuttle currents predicted by the model. These were measured at the boundary between the two plateaus, where insoluble products begin to form such as:

$3S_2^{2-} \leftrightarrow S_4^{2-} + 2S^{2-}$	Chemical

Disproportionation reactions would increase the concentration of S_4^{2-} at the cathode, which would require a reduction current to return these species back to S_2^{2-}. This reduction current would then contribute to the negative current measured as shuttle. This suggested improvement was, however, not implemented.

Kumaresan *et al.* [33] developed a one-dimensional model for a Li-S cell, expanding the mechanistic scheme to include both electrochemical reactions and chemical precipitation reactions, multi component transport phenomena in the porous electrode, and separator (assuming dilute solution theory) and charge transfer kinetics based on the Butler-Volmer equation. The model further allows for changes of porosity and active surface area in the cathode and separator, as a result of polysulfides dissolution and precipitation. The reactions considered are:

$Li \leftrightarrow Li^+ + e^-$	Electrochemical at Anode
$1/2S_8 + e^- \leftrightarrow 1/2S_8^{2-}$	Electrochemical at Cathode
$3/2S_8^{2-} + e^- \leftrightarrow 2S_6^{2-}$	Electrochemical at Cathode
$S_6^{2-} + e^- \leftrightarrow 3/2S_4^{2-}$	Electrochemical at Cathode
$1/2S_4^{2-} + e^- \leftrightarrow S_2^{2-}$	Electrochemical at Cathode
$1/2S_2^{2-} + e^- \leftrightarrow S^{2-}$	Electrochemical at Cathode
$S_{8(l)} \leftrightarrow S_{8(s)}$	Chemical precipitation on charge
$2Li^+ + S_x^{2-} \leftrightarrow Li_2S_{x(s)}$	Chemical precipitation on discharge X = 8, 4, 2, 1

The model is able to predict the time and spatial evolution across an electrode pair (anode-separator-cathode) of the species concentrations during discharge, together with changes in the porosity of the separator and cathode, and the volume fraction of the different precipitates. While the model qualitatively reproduces essential features of a typical Li-S cell discharge profile, such as the dip between the voltage plateaus, its predictions are not validated against experimental results. In view of the complexity and the large number of parameters involved in the White model, Chen and Ghaznavi [34, 41] perform a comprehensive sensitivity analysis of this model. They vary the discharge rate, sulfur dissolution rate, cathode conductivity, precipitation rate constants, exchange current density, diffusion coefficients and initial sulfur content. The model predicts a very flat second plateau which differs from experiment. This is attributed to the model ignoring the insulating properties of the sulfur precipitate. Although the surface area of the cathode decreases during precipitation as a result of decreased porosity, it is assumed that all cathode surfaces are electrochemically active. The model is very sensitive to the choice of rate constants, which appear as assumed parameters. While the model predicts a capacity loss due to precipitation, the simulated voltage curves are not qualitatively comparable to experimental behaviour. The model has a further limitation in that it cannot simulate charge.

Neidhardt *et al*. [36] developed a generic framework for describing the spatial and time evolution of an arbitrary number of phases in electrochemical devices, as well as the effect of interfacial (electro-) chemistry and microstructure in a continuum description. The general framework was developed to include concentrated solution theory, but when applied to Li-S batteries, dilute solution theory was used. The model allowed for the precipitation of polysulfides at the various solid/liquid interfaces, where sulfur/electrolyte, carbon electrolyte and precipitate/electrolyte were tracked individually. Instead of using Butler-Volmer kinetics, they used potential dependant mass action kinetics to describe the rate of electrochemical reactions. A 1D model based on this framework [37] simulates charge-discharge voltage curves and impedance spectra.

The results indicated that the discharge behaviour of the Li-S cell is governed by the presence of solid reactant and product phases in exchange with the dissolved polysulfide anions. The model also predicted an asymmetric behaviour of phase formation and dissolution between discharge and charge, as well as high charge over-potentials. The model was not validated with experiment. In particular, we note that the simulated impedance spectrum suggested that the series resistance was significantly smaller than the charge-transfer resistance, which contradicts typical EIS measurements for Li-S cells [42, 43]. Later [38] the model was developed to be a fully reversible 1D model. A simple reaction mechanism was considered:

$Li \leftrightarrow Li^+ + e^-$	Electrochemical at Anode
$S_{8(l)} \leftrightarrow S_{8(s)}$	Chemical precipitation on charge
$S_8 + 4e^- \leftrightarrow 2S_4^{2-}$	Electrochemical at Cathode
$S_4^{2-} + 6e^- \leftrightarrow 4S^{2-}$	Electrochemical at Cathode
$2Li^+ + S_2^{2-} \leftrightarrow Li_2S_{(s)}$	Chemical precipitation on discharge

Despite this simple reaction chain, the model was able to reproduce the macroscopic effects of the polysulfide shuttle such as infinite charging at low C charge rate, loss of active material at the anode, low coulombic efficiency and capacity fade due to Li_2S precipitation at the anode. The model provides a functional base model for the performance of a Li-S cell.

Others have attempted to model Li-S capacity fade. Informed by a simple reaction chain, Risse *et al.* [48] propose a general degradation model for Li-S cells that accounts for capacity fade due to cycling. The discharge process is described by a Markov chain with four states associated with three phases: an active or 'living' phase formed by active sulfur and Li^+, a sleeping phase that can be converted to living phase as cycling advances, representing sulfur previously unreachable becoming active, and a dead phase containing the material rendered irreversibly inactive, such as through the formation of a passivation layer and insoluble salts. Conversions from one phase to another take place according to pre-defined transition probabilities, and the amount of material in each phase is evaluated after each charge/discharge cycle. The six model parameters are obtained by fitting predictions to quantitatively and qualitatively different capacity fade trends with cycling. The results are used to analyse the effect of various cathode materials on cell cycle life from the perspective of changes in the interaction between the active matter and the cathode structure.

A few simulation efforts concentrate on obtaining information on reaction energetics in different solvents. Such models can provide valuable information for experimental work, such as informing cell chemistry and help to design targeted experiments, but also feed in parameter values for mechanistic models. The density functional theory (DFT) study by Wang [49] estimates the probable structures of the various polysulfides in the reduction chain during a Li-S cell discharge. They find a chain-like structure to be favoured by S^{2-} and S_6^{2-}, while a cluster structure is energetically favoured by all others. They also retrieve the favourable thermodynamic tendency that leads to spontaneous discharge. Using their results, they propose a three-step reaction chain $S_8 \rightarrow S_4^{2-} \rightarrow S_2^{2-} \rightarrow S^{2-}$. As the last two steps occur at similar equilibrium potentials, the effect of temperature, not accounted for in the study, could make the two latter plateaus appear as one as in standard discharge curves. The model enables an analysis of the effect of electrolyte on the magnitude of the voltage plateaus: the lower the electrolyte dielectric constant, the higher the voltage curve during the discharge.

Vijayakumar *et al*. [50], combines absorption X-ray spectroscopy and magnetic resonance with DFT analysis to investigate the dissolution mechanism of lithium polysulfides and their stability in an aprotic solvent (DMSO). They conclude that the dissolution of high order polysulfides (n>6) is initiated by fast Li^+ exchange with solvent molecules in a dynamic solvation shell. Lower order polysulfides are shown to dimerize or cluster in structures where Li^+ acts as the bridging unit. As a result, the Li^+ cannot interact with the solvent molecules, leading to lower solubilities than for the higher

order polysulfides. The ubiquitous S_6^{2-} ions are found to undergo dissociation reactions producing highly reactive S_3 radical anions. These radicals could be essential to cell performance.

This review highlights the nascent stage of development the implementation of Li-S physical models is in, and will be discussed further in a later section.

Survey of mechanisms predicted by experiment

In 2012 Canas *et al.* [14] used the following mechanism to explain XRD results:

$S_{8(s)} \leftrightarrow S_{8(l)}$	30% initially dissolves
$2Li + S_{8(l)} \leftrightarrow S_8^{2-} + 2Li^+$	70% S_8 Consumed as the concentration in solution decreases. No crystalline S_8 remains >20% DOD
$2Li + 3/4S_8^{2-} \leftrightarrow S_6^{2-} + 2Li^+$	Liquid Phase
$2Li + 2/3S_6^{2-} \leftrightarrow S_4^{2-} + 2Li^+$	Liquid Phase
$2Li + S_4^{2-} \leftrightarrow 2S_2^{2-} + 2Li^+$	Liquid Phase
$2Li + 1/2S_2^{2-} \leftrightarrow S^{2-} + 2Li^+$	Liquid Phase
$2Li^+ + S^{2-} \leftrightarrow Li_2S_{(s)}$	At 60% DOD crystalline Li_2S is observed. Intensity increases to 100% DOD. Contrary to the findings of Nelson *et al.* [12]

As discussed above, XRD can only observe crystalline intermediates present at the start and end of the Li-S cell mechanism. Much of the (electro-) chemistry was at this time considered to occur in some linear fashion at the electrode/electrolyte interface. During charge, the Li_2S solid was detected from 0% to 50% SOC and S_8 was observed at >95% SOC. In the same year, Barchasz *et al*. [26] used *ex-situ* spectroscopic methods and HPLC, to probe the mechanism and proposed three complex steps for the discharge in the LiTFSI/TEGDME electrolyte system:

Step 1, *Ca.*2.4V v Li^+/Li, 279 mAh/g, Overall $S_8 + 2e^- \rightarrow S_6^{2-} + ¼S_8$

$S_8 + 2e^- \rightarrow S_8^{2-}$	Slow, electrochemical
$S_8^{2-} \rightarrow S_6^{2-} + ¼S_8$	Fast, Concurrent disproportionation
$S_6^{2-} \rightarrow 2S_3^{\bullet-}$	Disproportionation
$2S_6^{2-} \rightarrow S_5^{2-} + S_7^{2-}$	Disproportionation

Step 2, *Ca.* 2.1V v Li^+/Li, 140 mAh/g, Overall $4S_3^{\bullet-} + 2e^- \rightarrow 3S_4^{2-}$

$2S_6^{2-} + 2e^- \rightarrow 3S_4^{2-}$	Electrochemical
$2S_3^{\bullet-} \rightarrow S_6^{2-}$	Slow, Concurrent association
$2S_4^{2-} \rightarrow S_5^{2-} + S_3^{2-}$	Disproportionation

Step 3, *Ca.* 2V v Li^+/Li, 1256 mAh/g, Overall $S_4^{2-} + 6e^- \rightarrow 4S^{2-}$

$3S_4^{2-} + 2e^- \rightarrow 4S_3^{2-}$	Electrochemical
$2S_3^{2-} + 2e^- \rightarrow 3S_2^{2-}$	Electrochemical
$S_2^{2-} + 2e^- \rightarrow 2S^{2-}$	Electrochemical

Or

$S_4^{2-} + 2e^- \rightarrow 2S_2^{2-}$	Electrochemical
$S_2^{2-} + S_4^{2-} \leftrightarrow 2S_3^{2-}$	Association
$S_2^{2-} + 2e^- \rightarrow 2S^{2-}$	Electrochemical

This work identified the presence of many polysulfide species in solution due to disproportionation reactions. The precipitation of poorly soluble insulating short chain or low order polysulfides in step 3 was evidenced by HPLC. The results explained the incomplete sulfur active material utilisation, with step 3 providing only 700mAh/g of sulfur of the theoretical 1256mAh/g. ESR data identified a single sulfur radical, the opened form of the S_3 radical anion with an absorption at 617nm in the UV. The radical is involved in the reduction process, being produced in step 1 and consumed in step 2. In fact, the S_3 radical anion is proposed to be involved in two equilibria, one fast electrochemical reaction leading to the formation of S_4^{2-}, and the slower association to S_6^{2-} that is readily consumed making the S_6^{2-} a transient intermediate. The S_3 radical anion could not be detected below 1.95V. It was concluded that the mechanism involves complex and successive equilibria that may depend on the first reduction step, intermediate species stability, discharge/charge rate and electrolyte composition, and that the choice of solvent impacts the choice of mechanistic pathway.

The following year Cuisnier *et al.* [29] performed *in-operando* XANES, and for the first time verified and quantified spectral features, Figure 5. Upon charge, they observed the monotonic consumption of Li_2S accompanied by the formation of shorter chain polysulfides. S_6^{2-} was detected at the start of charge and increased throughout whilst S_4^{2-} appeared as a transient species allowing oxidation of Li_2S into the more stable Li_2S_6. The disappearance of Li_2S and Li_2S_4 coincided with the voltage rise signalling the final oxidation of S_6^{2-} to S_8.

Upon discharge, S_6^{2-} was detected in the initial discharge step, agreeing with *ex-situ* studies that observed the rapid disproportionation of S_8^{2-} to S_6^{2-} + 1/4S_8 or, more likely, S_6^{2-} and Li_2S_2 or S_2^{2-}. Disproportionation is also observed in a second step to S_4^{2-}, such that supersaturation (dip in the discharge profile) marks not only the end of S_8 consumption, but also the maximum concentration of polysulfides.

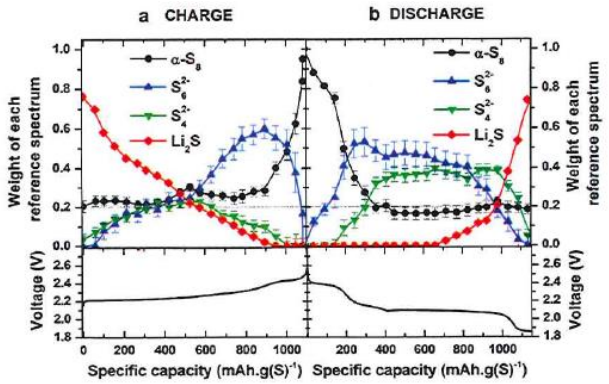

Figure 5 Evolution of sulfur k-edge XANES upon electrochemical cycling based on linear combination analysis at C/10 using 4 reference compounds whose weights are represented in the top panels. Reprinted with permission [29], Copyright 2013 American Chemical Society.

With a carbon composite cathode helping to retain polysulfides no Li_2S was observed at 2.1V until the second half of the plateau, attributed to supersaturation of Li_2S before finally crystallising. The final stage signals a steep increase in the fraction of Li_2S marked by a rise in resistance by impedance. Insoluble Li_2S_2 was not observed. In this case reduced sulfur utilisation was attributed to restricted or unreacted sulfur rather than the precipitation of Li_2S. This *in operando* insight into the mechanism provides a useful insight into the complex kinetics of the Li-S cell mechanism, although it should be understood that the mechanism may vary depending on cell design.

Kawase *et al.* [27] produced a similar polysulfide concentration map by *ex-situ* NMR and HPLC analysis of polysulfide derivatives, Figure 6. The range of polysulfides identified were increased and the discharge mechanism was summarised in 4 stages:

Stage 1 - High or 1st plateau 2.7 – 2.1V

$$S_8 + 2e^- \rightarrow S_8^{2-}$$

$$S_8 + 4e^- \rightarrow S_7^{2-} + S^{2-}$$

$$S_8 + 4e^- \rightarrow S_6^{2-} + S_2^{2-}$$

$$S_8 + 4e^- \rightarrow S_5^{2-} + S_3^{2-}$$

$$S_8 + 4e^- \rightarrow S_4^{2-} + S_4^{2-}$$

Stage 2 - High to low plateau 2.3 – 2.1V (Mid way on 2nd plateau)

$$S_8^{2-} + 2e^- \rightarrow S_6^{2-} + S_2^{2-}$$

$$S_8^{2-} + 2e^- \rightarrow S_5^{2-} + S_3^{2-}$$

$$S_8^{2-} + 2e^- \rightarrow S_4^{2-} + S_4^{2-}$$

$$S_7^{2-} + 2e^- \rightarrow S_4^{2-} + S_3^{2-}$$

$$S_6^{2-} + 2e^- \rightarrow S_3^{2-} + S_3^{2-}$$

$$S_5^{2-} + 2e^- \rightarrow S_3^{2-} + S_2^{2-}$$

$$S_4^{2-} + 2e^- \rightarrow S_2^{2-} + S_2^{2-}$$

Stage 3 - Low plateau 2.1V

$$S_3^{2-} + 2e^- \rightarrow S_2^{2-} + S^{2-}$$

Stage 4 - Low plateau <2.1V

$$S_2^{2-} + 2e^- \rightarrow S^{2-} + S^{2-}$$

This representation of the polysulfide mechanism provides a more complex picture, a general theme involving all of the polysulfides in a kinetic cascade from S_8 to Li_2S where, apart from the start and end, there is a complex dynamic of interconverting polysulfides through disproportionation and charge transfer. The Li_2S_3 species is dominant in the low plateau during charge and discharge. The exact concentration of species is dictated by cell design and solvent properties which also dictates sulfur utilisation. Charge was

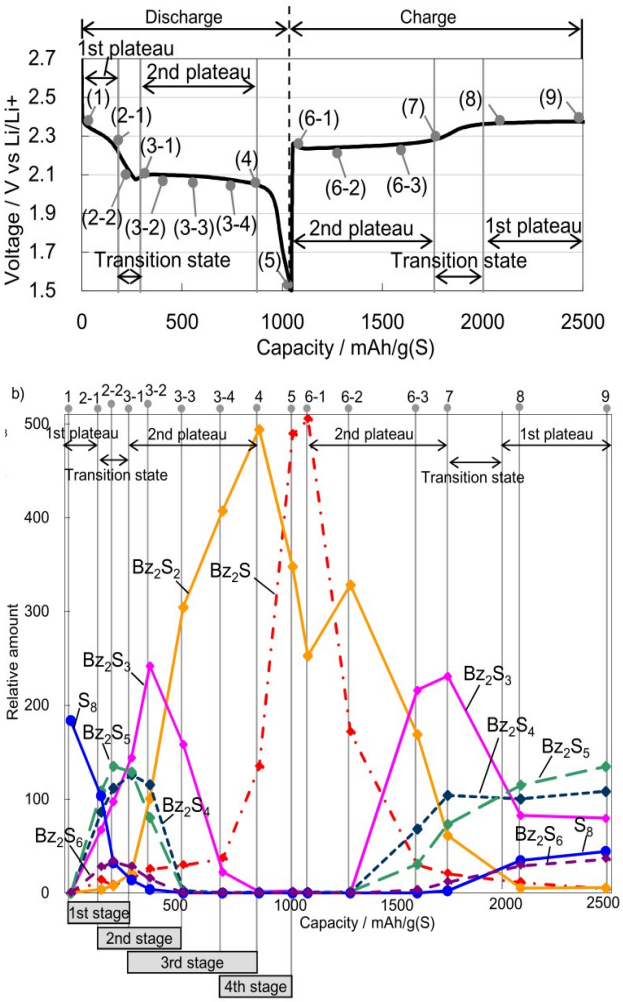

Figure 6 Above – Map of observation points during charge and discharge, Below – LC-MS mapped at the observation points. Adapted from [27] with permission from the Royal Society of Chemistry

observed as a reversal of discharge with the exception of a range of polysulfides resisting conversion to S_8; the reason was assumed to be due to the onset of polysulfide shuttle at the end of charge.

This technique did not observe radical species, however Lowe *et al.* [40] characterised the mechanism using *in-situ* XANES, and found the lower voltage plateau dominated by a specific set of sulfur species, not a sequential reduction of progressively more reduced polysulfides. The following dominating low plateau process was proposed:

$S_3^{\bullet -} + e^- \rightarrow S_3^{2-}$ Dominant low plateau reduction

$S_3^{2-} + S_n^{2-} \rightarrow S_6^{2-} + S_{n-3}^{2-}$ $3 < n < 8$

However, in order to balance charge n would need to be $4 < n < 8$.

$S_6^{2-} \leftrightarrow 2S_3^{\bullet -}$ Equilibrium

Then towards the end of discharge:

$S_3^{2-} + Li_2S_n \rightarrow Li_2S + S_{n+2}^{2-}$ $n = 2, 3$

This work provided further evidence of a sulfur reduction mechanism primarily controlled, and defined by, disproportionation reactions. They proposed that chemical equilibria of the polysulfides enable the reaction to approach chemical reversibility under appropriate conditions, but that these equilibria also limit the practical discharge capacity if the chemical equilibria maintain a distribution of incompletely reduced polysulfides. The authors made the point that chemical equilibria are governed by relative concentrations, not relative mass fractions. A shorter chain polysulfide will have a higher molar concentration than longer chain polysulfides. Thus there is a driving force to maintain a thermodynamic equilibrium even at the end of discharge. By example, they calculated that in an ideal cell 1672mAh/g capacity can be achieved. However, if 1 mol% of the sulfur species was trapped as S_8^{2-}, the accessible capacity drops more than 6% of full capacity.

Furthermore, they proposed that the presence of electrochemically inactive polysulfides can reasonably account for a significant fraction of the discrepancy from theoretical capacities. Thus, sulfur can be most fully and reversibly reduced under conditions where a high concentration of sulfur species exist in the diffusion layer of the electrode, and where chemical equilibria facilitate the formation of the S_3 radical anion that functions as a redox mediator. For example, the use of mesoporous carbon limits diffusion and maintains high local polysulfide concentrations for improved performance in some cell designs.

This mechanism for the low voltage plateau contrasts to that of Barchasz *et al*. [26] who proposed a similar mechanism involving the same species (step 2); the main difference being that Barchasz proposed an association of the S_3 radical anion followed by a reduction of the S_6 anion to give S_4:

$2S_3^{\bullet -} \rightarrow S_6^{2-}$ Slow, Concurrent association

$2S_6^{2-} + 2e^- \rightarrow 3S_4^{2-}$ Electrochemical

Whereas Abruña proposed an equilibrium and one electron reduction of the stable S_3 radical anion which concurs with the theoretical predictions of Assary *et al*. [3]:

$S_6^{2-} \leftrightarrow 2S_3^{\bullet -}$ Equilibrium

$S_3^{\bullet -} + e^- \rightarrow S_3^{2-}$ Dominant low plateau reduction

Kawase proposed an alternative more direct route to S_4^{2-} in the high plateau (Stage 1) although this is considered a simplification; the mechanism has been shown to be more accurately represented by multiple one electron transfers in cyclic voltammetry studies [21]:

$S_8 + 4e^- \rightarrow 2S_4^{2-}$

Lu *et al*. [22] probed the mechanism using a rotating disk electrode in different solvents. They also proposed a similar high plateau mechanism involving 6 steps:

Step 1 $S_8 + 2e^- \rightarrow S_8^{2-}$

Step 2 $S_8^{2-} + 2e^- \rightarrow S_8^{4-}$

Step 3 $S_8^{4-} \rightarrow 2S_4^{2-}$

Step 4 $S_8^{2-} \rightarrow S_6^{2-} + 1/4S_8$

Step 5 $S_6^{2-} \leftrightarrow 2S_3^{\bullet -}$

Step 6 $2S_4^{2-} \rightarrow$ [associations] $\rightarrow 6/7S_8^{2-} + 8/7S_1^{2-}$

In this mechanism, S_8 undergoes a sequential four electron reduction and disproportionation (step 1, 2 & 3) or disproportionation to S_6^{2-} (step 4), which is in equilibrium with the S_3 radical anion (step 5). Sulfur in step 4 is further reduced. It is proposed that reactions 1-3 occur in any solvent (*cf.* DOL/DME) whereas reaction 4 and 5 only occur in electron pair donor solvents with high dielectric such as DMSO, that can stabilise radicals. They then propose that reducible high plateau species such as S_8 and S_8^{2-} are formed by association such as:

$S_2^{2-} + S_7^{2-} \rightarrow S_8^{2-} + S^{2-}$

However the detail was not elucidated. In this mechanism, the presence of a dominant low plateau reduction step as proposed by others is not considered. However, the principle is the same in that the mechanism is dominated by chemical association and dissociation reactions that occur away from the electrode surface, whilst a smaller number of preferred redox reactions occur at the electrodes due to polysulfide dissolution and diffusion. Also, the common theme exists that the nature of the solvent determines the nature of the mechanism.

Assary *et al.* [3] performed a theoretical high level quantum chemical study, and determined the reduction potentials of lithium polysulfides and polysulfide molecular clusters, the energetics of

disproportionation and association reactions of likely intermediates and of their reactions with tetraglyme. They concluded that for the fragmentation of S_8 into two fragments the relative stability is $S_8 > S_6$ and $S_2 > S_5$ and $S_3 > 2S_4$. For the fragmentation of Li_2S_8 the formation of Li_2S_6 and Li_2S_4 is exergonic (favourable) while further fragmentation of Li_2S_6 and Li_2S_4 are endergonic (unfavourable) in solution. The reduction potential of S_2 occurs at 2V with respect to Li/Li^+, whilst other polysulfides and lithium sulfides except Li_2S_3 and Li_2S_2, occur at 2.5 – 2.0V. Reductions of Li_2S_3 and Li_2S_2 occur at 0.5 and 0.06V respectively and are not reduced under Li-S cell operating conditions. Based on a full assessment of the Gibbs free energies of polysulfides, the results explain the existence of major intermediates S_2^{2-}, S_3^{2-}, S_4^{2-} and the S_3 radical anion, which is in general agreement with experimental data. Analysis of anions in solution indicates that the most abundant intermediate upon complete utilisation of S_8^{2-} is S_3^{2-} whilst the products are Li_2S and Li_2S_2 upon discharge. The study suggests that tetraglyme is vulnerable to nucleophilic attack from Li_2S_2 and Li_2S_3 species in solution, with Li_2S_3 being the most reactive, suggesting long term instability of ethers in the presence of Li_2S_2 and Li_2S_3.

Based on computed reduction potentials and free energies of reactions, a detailed mechanism was proposed to explain the likely reaction network of polysulfides (S_8^{2-}), as well as the dissolution of lithium polysulfides (Li_2S_8) in solution, Figure 7. This study goes some way to clarifying the allowed inter-conversions from which any subset may occur, depending on cell design and the choice of electrolyte. It is interesting to note that on discharge all allowed reactions from a thermodynamics perspective are either reductions or dissociation. They are not complex multi species associations as commonly proposed by many authors attempting to explain experimental results.

Formation of Li_2S_8

Reactant	Reactions→							Product
S_8	S_8^{1-}	S_8^{2-}	$2Li^+$	Li_2S_8	$Li_2S_8^{2-}$	$2Li^+$	Li_2S_7	Li_2S
				Li_2S_8	$Li_2S_8^{2-}$	$2Li^+$	Li_2S_6	Li_2S_2
				Li_2S_8	$Li_2S_8^{2-}$	$2Li^+$	Li_2S_5	Li_2S_3
				Li_2S_8	$Li_2S_8^{2-}$	$2Li^+$	Li_2S_4	Li_2S_4
				Li_2S_7	$Li_2S_7^{2-}$	$2Li^+$	Li_2S_6	Li_2S
				Li_2S_7	$Li_2S_7^{2-}$	$2Li^+$	Li_2S_5	Li_2S_2
				Li_2S_7	$Li_2S_7^{2-}$	$2Li^+$	Li_2S_4	Li_2S_3
				Li_2S_6	$Li_2S_6^{2-}$	$2Li^+$	Li_2S_5	Li_2S
				Li_2S_6	$Li_2S_6^{2-}$	$2Li^+$	Li_2S_4	Li_2S_2
				Li_2S_5	$Li_2S_5^{2-}$	$2Li^+$	Li_2S_4	Li_2S
				Li_2S_5	$Li_2S_5^{2-}$	$2Li^+$	Li_2S_3	Li_2S_2
				Li_2S_4	$Li_2S_4^{2-}$	$2Li^+$	Li_2S_3	Li_2S
				Li_2S_4	$Li_2S_4^{2-}$	$2Li^+$	Li_2S_2	Li_2S_2

(b) Lithium polysulfides

Reactant	Reactions→				Product
S_8^{2-}	R_9	S_3^{1-}	S_3^{2-}	$2Li^+$	Li_2S_3
S_8^{1-}	R_{20}	S_2^{1-}	S_2^{2-}	$2Li^+$	Li_2S_2
S_8^{2-}	R_{12}	S_4^{1-}	S_4^{2-}	$2Li^+$	Li_2S_4
S_8^{1-}	R_{20}	S_6	S_6^{1-}	S_6^{2-}	
S_6^{1-}	R_{34}	S_2^{1-}	S_2^{2-}	$2Li^+$	Li_2S_2
S_6^{1-}	R_{35}	S_4^{1-}	S_4^{2-}	$2Li^+$	Li_2S_4
S_6^{2-}	R_{25}	S_3^{1-}	S_3^{2-}	$2Li^+$	Li_2S_3
S_4^{2-}	R_{42}	S_3^{2-}		$2Li^+$	Li_2S_3

(a) Polysulfide anions

Figure 7 Proposed schematic representation of reduction pathways for (a) polysulfide anions and (b) lithium polysulfides in Li-S systems, A mechanism proposed from the computed free energies of various reaction and reduction potentials, Assary *et al*. [3]. In (a) each row represents the mechanism of formation of small polysulfides (S_n, n≤3) from longer chain sulfides (S_n, 4≥ n ≤8). In each row, adjacent yellow cells represent electrochemical processes, cells with R_n (green cells) represent chemical transformations shown in table 4 of the original article and blue cells (with $2Li^+$) represent the addition of 2 lithium ions. (b) Each row represents the mechanism of formation of small chain lithium sulfides (Li_2S_n, n≤3) from lithium polysulfides (Li_2S_n, n≤8). In each row adjacent yellow cells represent electrochemical (2 electron reduction) reactions. In each row, the green cell represents reaction with $2Li^+$ ions and subsequent fragmentation to give the species shown in the red cell. The species in the red cell undergoes further reaction sequences including reduction, addition of lithium ion, and subsequent fragmentation to form the species in the final column, which are shown in subsequent rows. Reprinted with permission [3]. Copyright 2014 American Chemical Society

Wang *et al.* [31] analysed the role of the S_3 radical anion in more detail using *in situ* EPR. The concentration of sulfur radicals was found to change periodically at different potentials. During discharge in coin cells with a DOL/DME electrolyte, the concentration of the S_3 radical anion increased fast and reached a maximum at 2.0V. As the potential decreased further, the concentration of the radical also decreased indicating its consumption at lower potentials. Upon charge the concentration of the radical continued to decrease and plateaued between 2.0 and 2.75V, suggesting a temporal balance between consumption and generation. A sharp drop of radical concentration is observed towards the end of charge, and a similar delay in radical concentration response is seen as the cell is again discharged. They detected the S_3 radical anion with all polysulfide species from Li_2S_8 to Li_2S_2 except in commercial Li_2S, such that nominally stoichiometric Li_2S_x is in fact a mixture in which S_6^{2-} and the S_3 radical anion co-exist, such that the S_3 radical anion was not consumed completely, and even appears in Li_2S_2. They proposed a three step mechanism for discharge:

Step 1 2.3V plateau (*cf.* Barchasz *et al*.)

$$S_8 + 2e^- \rightarrow S_8^{2-} \quad \text{Slow, electrochemical}$$

$$S_8^{2-} \leftrightarrow S_6^{2-} + \tfrac{1}{4}S_8 \quad \text{Fast, Concurrent disproportionation}$$

$$S_6^{2-} \leftrightarrow 2S_3^{\bullet -} \quad \text{Chemical equilibrium}$$

Step 2 2.1V - 2.3V Liquid to semi-solid
(Li_2S_4 semi solid in DOL/DME, (Dip))

$$S_8^{2-} + 2e^- \rightarrow S_4^{2-} + S_4^{2-}$$

$$S_6^{2-}(S_3^{\bullet -}) + e^- \rightarrow 3/2S_4^{2-}$$

Step 3 2.1V Plateau

$$S_4^{2-} + 2e^- + 4Li^+ \rightarrow 2Li_2S_2$$

$$Li_2S_2 + 2e^- + 2Li^+ \rightarrow 2Li_2S \quad \text{Electrochemical}$$

$$S_4^{2-} \leftrightarrow 3/5S_6^{2-}(S_3^{\bullet -}) + 2/5S^{2-}$$

$$S^{2-} + 2Li^+ \rightarrow Li_2S \quad \text{Chemical}$$

It is proposed (step 1) that at the end of the 2.3V first plateau $S_6^{2-}(S_3^{\bullet -})$ and S_8 reach equilibrium. The dominant electrochemical reaction in this region is suggested to be the two-phase transition between S_8 and Li_2S_8, whilst conversion to Li_2S_6 is mainly a chemical step. Then in step 2, S_8^{2-} and S_6^{2-} are electrochemically reduced to S_4^{2-}. Li_2S_4 is a semisolid in this electrolyte and causes a dip in voltage. As the voltage decreases it is proposed there is further electrochemical reduction of S_4^{2-} to S_2^{2-} and S^{2-} whilst chemical disproportionation of S_4^{2-} into S^{2-} and S_6^{2-} occurs concurrently. The electrochemically derived Li_2S depends on current density and cut off voltage, while chemically formed Li_2S depends on the electrolyte and cell design. At the end of discharge a new equilibrium is formed between S_4^{2-}, the S_3 radical anion, S_6^{2-}, Li_2S_2 and Li_2S with Li_2S_2 and Li_2S dominant. Thus, the radical concentration does not drop to zero in agreement with Abruña *et al*, meaning that if the discharge is terminated earlier by adjusting the cut off voltage, less insulating Li_2S forms in the equilibrium, improving cyclability.

As recognised by Lowe *et al.* this is an important feature for charge. During discharge a distinct transition (dip) between 2.3 and 2.1V is observed, which disappears upon charge. In addition, upon charge the voltage jumps quickly to reach a long plateau at 2.3V. They note that despite the current density, the polarisation of charge curves changes little from C/50 to C/5. Another transition occurs at 2.4V from S_8^{2-} to S_8. They propose a 3 step charge mechanism:

Step 1 Chemical equilibrium after discharge

$$2/5Li_2S + 3/5S_6^{2-}(S_3^{\bullet -}) \leftrightarrow S_4^{2-} + 4/5Li^+$$

$$1/5Li_2S_2 + 3/5S_6^{2-}(S_3^{\bullet -}) \leftrightarrow S_4^{2-} + 2/5Li^+$$

Step 2 Plateau after a sharp rise to 2.3V

$$2S_4^{2-} - 2e^- \leftrightarrow S_8^{2-}/S_8$$

Step 3 2.4V Plateau

$$S_8^{2-}/S_6^{2-} - 2e^- \leftrightarrow S_8$$

Li_2S and Li_2S_2 equilibrates with the S_3 radical anion and Li_2S_6 to form S_4^{2-}, which will immediately form S_8^{2-}/S_6^{2-} directly due to the conversion of a semisolid to liquid. Once S_8^{2-}/S_6^{2-} forms, more S_3 radical anion can be generated to drive the chemical reactions that use the insoluble Li_2S/Li_2S_2. A constant concentration of the S_3 radical anion is maintained during charge until the final conversion to S_8. However, in order to achieve the trend shown in the XANES data in Figure 3, step 1 would be expected to be fast, and step 2 slow, which might be expected from an association reaction making the S_4^{2-} a transient intermediate in the charge mechanism.

Cuisnier *et al.* [30] investigated the role of the S_3 radical anion *in operando* using XANES. They concluded that radicals are not stabilised in glyme based electrolytes and are not present in a measurable concentration (<<5% in DOL/DME over *Ca.* 5 minutes), whilst they are in electron pair donor solvents (up to 25% in DMA), where the S_3 radical anion is in high concentration but reacts less with the solvents (common EPD solvents are not stable against lithium however). The stability of the electrolyte solvent against metallic lithium, and the presence of un-stabilised radicals, are both valid degradation mechanisms leading to electrolyte depletion. They were able to show that cyclic glymes undergo nucleophilic attack by sulfur radicals, and although the concentration is low in DOL/DME electrolytes, DOL decomposition is likely with extended cycling. DMSO, on the other hand, was shown to be stable against radicals but unstable against lithium. The S_3 radical anion was detected as soon as discharge started and reached a maximum at 340mAh/g and persisted up to 850mAh/g in DMA. While a fit of the data was possible with four species S_8, S_4^{2-}, S_3 radical anion and Li_2S, the exact species could not be discriminated in detail. The following

mechanism is used to explain the results; the S_4^{2-} is used to represent the sum of polysulfide dianions:

Step 1 2.7V plateau (*cf.* Barchasz *et al*.)

$$S_8 + 2e^- \rightarrow S_8^{2-}$$

$$S_8^{2-} \leftrightarrow S_6^{2-} + \tfrac{1}{4}S_8$$

$$S_6^{2-} \leftrightarrow 2S_3^{\bullet-} \qquad \text{Chemical equilibrium}$$

Step 2 <2.2V

$$S_3^{\bullet-} + e^- \rightarrow S_3^{2-}$$

$$2S_3^{2-} + S_3^{\bullet-} \rightarrow 3S_4^{2-}$$

$$S_8^{2-} + 2e^- \rightarrow 2S_4^{2-}$$

Step 3 <2.2V

$$S_4^{2-} + 1/4S_8 \rightarrow 2S_3^{\bullet-}$$

$$S_4^{2-} + 6e^- \rightarrow 4S^{2-}$$

$$S^{2-} + 1/4S_8 \rightarrow 4S_3^{2-}$$

In step 1 the S_4 radical anion has never been detected in DMA. In EPD solvents the main product is the S_3 radical anion. In step 2 the maximum concentration of the S_3 radical anion coincides with the voltage drop from 2.7 to 2.2V. In step 3 medium length polysulfides are re-oxidised to the S_3 radical anion by S_8 or Li_2S_8 so that the reduction of the S_3 radical anion concentration during discharge must indicate full utilisation of elemental sulfur. Reduction continues until the final discharged state is composed of short chain Li_2S_n and Li_2S.

Cuisnier *et al.* made the interesting point that the use of low volatility EPD solvents which facilitate the phase transfer of Li_2S would be beneficial in catholyte-type or redox flow type batteries, where Li_2S deposition is controlled by surface interactions, but that these solvents would be detrimental when trying to limit diffusion by physically entrapping sulfur species in mesoporous carbons. Instead a highly adsorptive electrode material with a highly dissociative solvent could be advantageous to increase sulfur utilisation. In the same way constraining polysulfide release from the cathode matrix may do the same if solvents are used to impede chemical equilibria. The design of cathode and electrolyte are intimately linked and must be considered as one system to achieve maximum capacity.

Perspectives on the Li-S mechanism

Analytical Studies

It is clear that the elucidation of the mechanism for the Li-S battery is a current and exciting topic with growing interest from the academic community. However, this is a complex problem, rather like the blind man trying to identify the proverbial elephant. No single technique is capable of identifying and quantifying the polysulfide species, so the puzzle must be pieced together from multiple sources.

It is also clear that *in-situ* and *in-operando* methods are critical to understanding the dynamics of the mechanism throughout discharge and charge. Yet such results are likely to be sensitive to cell design, both for the choice of electrolyte and also the complimentary choice of cathode and other cell components. Ex-situ methods, by their nature, are prone to greater error given the propensity for polysulfides to interconvert through facile association and dissociation reactions. Charge has been much less studied than discharge and yet is unlikely to be a simple reversal of the discharge process. The fidelity of cell design must be taken into account when making general conclusions about the Li-S mechanism from experiment.

To date, the experimental analysis does not take into account spatial aspects of the Li-S mechanism, as chemically much of it is envisaged in the electrolyte whilst electrochemical reactions occur at surfaces. The study of heterogeneous chemical reactions catalysing polysulfide inter-conversions at the electrode surfaces are absent from the literature. There is a need to understand better the role that separators, catholytes, cathode matrices and binder systems play, in addition to the electrolyte systems, in determining the exact Li-S mechanism. By example, the different stabilities of the proposed radical anion intermediate depending on concentration, dielectric, electron donor properties and such like that determine the radical or anionic nature of the mechanism.

The available resolution of analytical techniques struggles to account for all of the possible polysulfide species taking part in the Li-S mechanism. Assary *et al.* [3] provide a theoretical tool box of possible species and their reactions but, to date, experimental studies focus on a core subset of theoretical possibilities. It is not clear whether this is because they are the preferred species in the cell design under consideration, whether they are simplifications, or whether it is because of the limitations of the analytical methods in seeing these other possible species.

Looking forward it is clear there is a need to coordinate and focus on cell design and its components when interpreting the results of analytical experiments in order to classify the modes of the mechanism that may exist. For example, do the anions or radicals mostly dominate the mechanism and what are the low and high plateau species concentrations in solution? (is sulfur constrained in the cathode or does sulfur fully dissolve during the upper plateau?).

Advancing the subject to improve spatial understanding of the mechanism may help to focus the efforts of materials research, whilst improved temporal understanding may advance predictive modelling efforts.

The proposed mechanisms used to explain experimental results, although detailed, present a number of issues and more often every

possibility and none. Cyclic voltammetry [21] has shown that the first reduction step (S_8 to S_8^{2-}) proceeds via 2 x 1 electron transfer rather than a 1 x 2 electron transfer. In fact, all of the reductions are likely to be 1 electron yet, with the exception of discussions on the S_3 radical anion, reductions are nearly always shown as 2 or even more implausible four electron transfers. Assary *et al.* [3] has presented a theoretical study of the most likely polysulfide inter-conversions, the discharge is thought to be dominated by binary dissociation. It is hard to imagine the likelihood of some of the more complex suggestions involving the association of multiple species, for example, $S_8^{2-} \rightarrow S_6^{2-} + ¼S_8$ is commonly used. It implies that four fragments of S_2 combine to reform S_8 in some cases, although we believe the formation of Li_2S_2 or $2Li_2S$ is more likely. Equally, if the equation were balanced, as many are not, it would imply $4S_8 \rightarrow 4S_6^{2-} + S_8$, in which case dissociation would require a complex reaction involving $4S_8$ rings rearranging to form 4 more stable S_6 rings and the remainder forming the less stable S_8 structure. In another example, two species have been proposed to take part in an electrochemical reaction to give 3 species: $2S_6^{2-} + 2e^- \rightarrow 3S_4^{2-}$, which seems unnecessarily complex when simpler more plausible alternatives exist, that would be favoured by Occam's Razor. There is an opportunity to focus efforts on elucidating in greater detail the critical steps that can better inform both modelling efforts and materials research, not unlike determining metabolic pathways in organic systems.

Materials Research

The current understanding of the mechanism can help to direct materials research today. It is clear the electrolyte is critical to the performance of the cell, firstly from a mechanistic perspective, but also from the point of view of materials compatibility.

Electrolytes must be designed to promote radical redox mediation by the stable S_3 radical anion. It is essential to recognise that to achieve the theoretical maximum capacity, some solubility of Li_2S is required to increase the accessible capacity and to decrease the equilibrium concentration of intermediate polysulfides in solution at 100% DOD. A high concentration of sulfur species is required in the diffusion layer to promote chemical equilibria that form the S_3 radical anion [40] that acts as a redox mediator. Radicals are stabilised in electron pair donor solvents and in ethers with high numbers of coordinating Oxygen's, whilst cathode design modifies the retention of polysulfides to increase diffusion layer concentrations.

Conversely, electrolyte components have to be stable to the harsh environment in the Li-S cell and much effort is placed on understanding and modifying the SEI of the lithium metal anode to address this issue. However, analytical studies highlight that the anode is only one degradation mechanism and Cuisinier *et al.* have shown that common solvents (ethers, glymes) used in research today are reactive towards the crucial radical intermediates required for high sulfur utilisation. This points the way to the need to develop new classes of electrolytes for use in Li-S cells. Electrolytes that remain stable in the presence of radicals and that solubilise sufficient polysulfides in order to promote association and dissociation reactions in the cathode or catholyte in association with a stable anode SEI.

For materials research it is not only important to coordinate and focus on cell design when interpreting the results of materials research but also, as Urbonaite and Novák [51] reported, that even the seemingly unimportant experimental parameters strongly influence performance. They need to be disclosed clearly to enable comparison and reproduction of results such as the particle size of the sulfur for instance.

Physical modelling

It is clear that there is a paucity of developed Li-S models and these models only qualitatively describe some features of Li-S cells. They are not able to explain some of the latest experimental results. This new mechanistic understanding from the experimental community, although imperfect, provides an excellent opportunity to improve the physical models of the Li-S cell. Models developed with the Li-ion mechanism in mind are dominated by electrochemistry at the electrode surfaces. Li-ion systems use intercalation, wherein the lithium ions are inserted and extracted from a host crystal species, and sometimes exhibit phase change. However, it is clear from the preceding discussion that in order to capture the complex features of Li-S with any fidelity the chemistry of the polysulfide mechanism must be included. Li-S systems operate through electrochemical and chemical reactions in the solution phase and hence should be treated very differently. Likewise there is need for models to be developed to better understand lithium anode degradation and SEI design, so as to aid materials research. More detailed structural models are also needed, to take better into account changes in viscosity and porosity during cycling, since this affects accessible capacity.

It is clear that the understanding of the mechanisms of Li-S cells is still limited today from an experimental perspective, and that there are limitations on the choice of materials from a materials research perspective. Therefore models have to be developed making use of incomplete experimental data. Where values for key parameters such as rate constants of the polysulfide reactions are not available, fitting of model prediction's to experimental data will be required. It must also be recognised that there is significant computational cost to model the full complexity of the proposed mechanisms.

It is however possible to identify a number of generic features that the next generation of Li-S models should include to better represent the unique features of a Li-S cell. These include:

- Charge transfer at the solid/electrolyte interface
- Dissolution and precipitation at the end of charge and discharge, and Li_2S precipitation during discharge at the start of the low plateau
- The possibility of alternative mechanistic pathways and the dominance of various polysulfide species depending on the operating conditions and design of the cell
- Mechanistically a predominantly disassociatiative mechanism upon discharge with a dominant

electrochemical cycle in the low plateau based at least around the stable $S_6^{2-} \leftrightarrow 2S_3^{\bullet-}$ equilibrium
- Asymmetry between charge and discharge
- Model variables to account for the nature of the electrolyte e.g. a radical or anionic character to the mechanism
- The impact of viscosity, conductivity and solubility of species in the electrolyte on the cell resistance
- The concentration of polysulfide species in the diffusion layer to promote chemical equilibrium
- Spatial and temporal resolution of the evolving morphology; for example the changing electrochemical surface area and composition of the cathode and anode, as well as the composition on reformation and porosity of the cathode, separator and anode
- Inaccessible capacity from trapped polysulfide species in electrolyte
- Rates of irreversible capacity loss from materials degradation such as changes in the anode surface area during charge and discharge, SEI formation and reformation
- Rates for polysulfide shuttle and self-discharge as a function of current and temperature, with the possibility to mimic the effects of additives such as shuttle inhibitors.

Although the actual mechanism is more complex, a simplified working model of the discharge mechanism is summarised in Figure 8 that addresses many of the required features. At the cathode/anode surface all available polysulfides (di-anions, anions, radicals and neutral species) and lithium salts take part in surface enabled electrochemical and chemical reactions.

In solution, chemical association and dissociation reactions maintain a working concentration of electrochemically active intermediates until polysulfide phase transitions take place. These precipitation, crystallisation and dissolution processes give rise to an increase in the cell internal resistance which hinders further activity. Intermediate species remaining in solution are 'trapped' at their equilibrium concentrations until subsequent cycles, contributing to variable reversible capacity. Depicted as high and low plateau regions electrochemically, the chemical transitions are considered as a continuous multi-species system. The system is modified by controlling porous structure and the choice of solvents and additives to modify the SEI, ion mobility and rate of chemical reaction.

The charge mechanism is expected to be similar, but is unlikely to be an exact reversal of the discharge process and is likely to be more direct as suggested by Lowe *et al.* [13]. There are key differences between charge and discharge. For example, upon charge the electrochemical surface is cleaned by association reactions involving S^{2-} and some other polysulfide species, until the very end of charge where S_8 begins to precipitate and requires association; conversely the discharge is dominated by dissociation reactions. This may mean charge has a more electrochemical than chemical character. Based on the comparison with Li_2S batteries, the role of intermediate redox mediators is likely to be critical in catalysing the start of charge, and addresses the issue of Li_2S solubility which prevents some models from charging [33].

Conclusions

This review summarises the current state of the mechanistic understanding of Li-S batteries, from the twin perspective of experimental analytical studies and the development of physical models. Important limitations are discussed highlighting scope for further work in the field. The review concludes with a proposal for a simplified model of the Li-S mechanism, the features of which can be used as the basis of new higher fidelity physical models, to accurately reproduce more of the unique aspects of Li-S chemistry that determine its performance. Such models could then be used to inform materials research and to provide greater understanding for the uptake of Li-S batteries in real world applications.

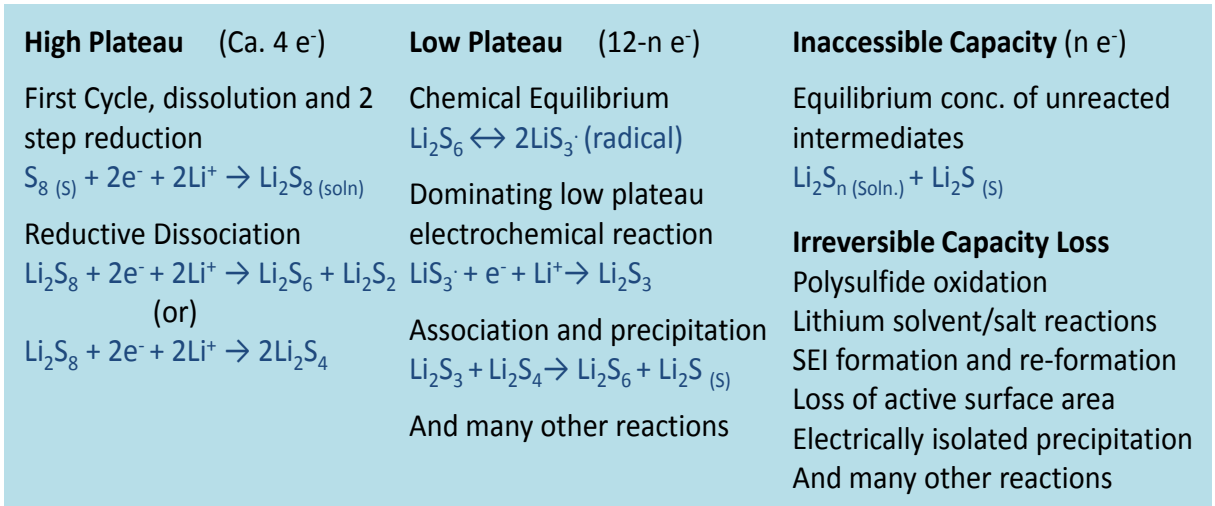

Figure 8. Representative reaction mechanism for the discharge of a Li-S cell

Acknowledgements

The authors would like to thank Innovate UK and the Engineering and Physical Sciences Research Council in the UK for funding this work under the Revolutionary Electric Vehicle Battery Project (RevB, #101573, EP/L505298/1).

References

1 Xu, W., Wang, J., Ding, F., Chen., Nasybulin, E., Zhang, Y., and Zhang, J. G. *Energy Environ. Sci*., 2014, **7,** 513
2 Zu, C., Manthiram, A. *J. Phys. Chem. Lett.* 2014, **5**, 2522-2527
3 Assary, R. S., Curtiss, L.A., and Moore, S. *J. Phys. Chem. C*. 2014, **118**, 11545-11558
4 Diao, Y., Xie, K., Xiong, S., and Hong, X. *J. Power Sources* 2013, **235,** 181
5 Xiong, S., Xie, K., Diao, Y., and Hong, X. J. Power Sources 2014, **246**, 840
6 Yeon, J. T., Jang, J. Y., Han, J. G., Cho, J., Lee, K. T., and Choi, N. S. *J. Electrochem. Soc*. 2012, **159**, A1308
7 Lécuyer, M., Gaubicher, J., Deschamps, M., Lestriez, B., Brousse, T., and Guyomard, D. *J. Power Sources* 2013, **241**, 249
8 Kim, C. S., Guerfi, a., Hovington, P., Trottier, J., Gagnon, C., Barray, F., Vijh, A., Armand, M., and Zaghib, K., *J. Power Sources* 2013, **241**, 554
9 Kang, S. H., Zhao, X., Manuel, J., Ahn, H. J., Kim, K. W., Cho, K. K., and Ahn, J. H. *Phys. Status Solidi* 2014, **211**, 1895
10 Dornbusch, D. A., Hilton, R., Gordon, M. J., and Suppes, G. J., *Ind. Eng. Chem.* 2013, **19**, 1968
11 Revolutionary Electric Vehicle Project (Innovate UK, RevB, Project #101573)
12 Nelson, J., Misra, S., Yang, Y., Jackson, A., Liu, Y., Wang, H., Dai, H., Andrews, J. C., and Toney, M. F. *Journal of the American Chemical Society*, 2012, **134,** 6337-6343
13 Lowe, M. A., Gao, J., and Abruña, H. D. *RSC Advances*, 2014, **4**, 18347-18353
14 Canas, N. A., Wold, S., Wagner, N., and Friedrich, K. A. *Journal of power sources* 2013, **226**, 313-319
15 Walus, S., Barchasz, C., Colin, J-F., Martin, J.-F., Elkaim, E., Lepretre, J.-C., and Alloin, F. Chemical Communications 2013, **49**, 7899-7901
16 Choi, N, S., Chen, Z., Freunberger, S. A., Ji, X., Sun, Y. K., Yushin, G., Nazar, L. F., Cho, J., and Bruce, P. G. *Angwandte Chemie – International edition* 2012, **51**, 9994-10024
17 Zhaoqing, J., Kai, X., and Xiaobin, H. *Acta Chimica Sinica* 2014, **72**, 11-20
18 Bresser, D., Passerini, S., and Scrosati, B. Chemical Communications 2013, **49**, 10545-10562
19 Zhen-Dong, Y., Wei, W., Jiu-Lin, W., Jun, Y., and Yan-Na, N. Acat Physio-Chimica Sinica 2011, **27**, 1005-1016
20 Yin, Y, X., Xin, S., Guo, Y. G. and Wan, L. J. Angewandte Chemie-International Edition 2013, **52**, 13186-13200
21 Jung, Y., Kim, S., Kim, B. S., Han, D, H., Park, S. M. and Kwak, J. *International journal of electrochemical science* 2008, **3**, 566-577
22 Lu, Y. C., He, Q., and Gasteiger, H. A., Journal of physical chemistry 2014, **118**, 5733-5741
23 Schneider, H., Garsuch, A., Panchenko, A., Gronwald, O., Janssen, N., and Novák, P. *Journal of Power Sources* 2012, **205**, 420-425
24 Patel, M. U. M., Demir-Caken, R., Morcrette, M. Tarascon, J. M., Gaberscek, M., and Dominko, R. *Chem-SusChem Communications* 2013, **6**, 1177-1181
25 Cañas, N., A., Fronzek, D. N., Wagner, N., Latz, A., and Friedrich, K. A. *The journal of physical chemistry C* 2014, **118**, 12106-12114
26 Barchasz, C., Florian, M., Duboc, C., Lapretre, J. C., Patoux, S., and Alloin, F. Analytical chemistry 2012, **84**, 3973-3980
27 Kawase, A., Shirai, S., Yamoto, Y.,Arakawa, R., and Takata, T. *Physical Chemistry Chemical Physics* 2014, **16**, 9344-9350
28 Gao, J., Lowe, M. A., Kiya, Y., and Abruña, H. D. *Journal of Physical Chemistry C* 2011, **115**, 25132-25137
29 Cuisnier, M., Cabelguen, P. E., Evers, S., He, G., Kolbeck, M., Garsuch, A., Bolin, T., Balasubramanian, M., and Nazar, L. F. Journal of Physical Chemistry Letters 2013, **4**, 3227-3232
30 Cuisinier, M., Hart, C., Balasubramanian, M., Garsuch, A., and Nazar L. F. *Adv. Energy Mater.* 2015, **1401801**, 1-6
31 Wang, Q., Jianming, Z., Wailter, E., Huilin, P., Lv, L., Zuo, P., Chen, H., Deng, Z. D., Liaw, B. Y., Yu, X.., Yang, X., Zhang, J. G., Liu, J., Xiao, *J. Journal of the electrochemical society* 2015, **162**, A474-A478
32 Mikhaylik, Y. V., and Akridge, R. *Journal of the electrochemical society* 2004, 151, A1969-A1976
33 Kumaresan, K., Mikhaylik, Y., and White, R. E. *Journal of the electrochemical society* 2008, **155**, A576-A582
34 Ghaznavi, M., and Chen, P. Journal of power sources 2014, **257**, 394-401
35 Schneider, H., Gollub, C., Weib, T., Kulisch, J., Leitner, K., Schmidt, R., Safont-Sempere, M., Mikhaylik, Y., Kelley, T., Scordilis-Kelley, C., Laramie, M., and Du, H., ,*Journal of the Electrochemical Society*, 2014, **161,** A1399-A1406
36 Neidhardt, J. P., Fronczek, D. N., Jahnke, T., Danner, T., Horstmann, B., and Bessler, W. G. *Journal of the electrochemistry society* 2012, **159**, A1528-A1542
37 Fronczek, D. N., Bessler, W. G. *Journal of power sources* 2013, **244**, 183-188
38 Hofmann, A. F., Fronczek, D. N., Bessler, W. G. *Journal of power sources* 2013, **259**, 300-310
39 Moy, D., Manivannan, A., and Narayanan, S. R. *Journal of the electrochemical society* 2015, **162**, A1-A7
40 Lowe, A. M., Gao, J., and Abruña, H. D., *RSC Adv.* 2014, **4**, 18347-18353
41 Ghaznavi, M., and Chen. P., *Electrochimica Acta*. 2014, **137**, 575-585
42 Canas, N, A., Hirose, K., Pascucci, B., Wagner, N., Friedrich, K. A, and Hiesgen, R. *Electrochimica Acta*. 2013, **97**, 42-51
43 Zhaofeng, D., Zhang, Z., Lai, Y., Liu, J., Li, J., and Liu, Y. *Journal of the Electrochemical Society* 2013, **160**, A553-A558
44 Macdonald, J. R. and Johnson, W. B. (2005) *Fundamentals of Impedance Spectroscopy* in E. Barsoukov, J. Ross Macdonald (Eds.), *Impedance Spectroscopy: Theory, Experiment and Applications* (2nd Ed.). , John Wiley & Sons, Inc., Hoboken, New Jersey
45 Kolosnitsyn, V. S., Kuzmina, E. V., Karaseva, E.V., Mochalov S.E. *Russian Journal of Electrochemistry*, 2011, **47(7)**, 793-798
46 Wu, H-L., Huff, L. A. and Gewirth, A. A. *App/. Mater. Interfaces* 2015, **7**, 1709-1719

47 Gorlin, Y., Siebel, A., Piana, M., Huthwelker, T., Jha, H., Monsch, G., Kraus, F., Gasteiger, H. A. and Tromp, M. *Journal of the electrochemical society* 2015, **162(7)**, A1146-A1155
48 Risse, S., Angioletti-Uberti, S., Dzubiella, J., and Ballauff, M. *Journal of Power Sources* 2014, **267**, 648-654
49 Wang, L., Zhang, T., Yang, S., Cheng, F., Liang, J., and Chen, J. *Journal of Energy Chemistry* 2013, **22**, 72-77
50 Vijayakumar, M., Govind, N., Walter, E., Burton, S. D., Shukla, A., Devaraj, A., and Thevuthasan, S. *Physical Chemistry Chemical Physics* 2014, **16**, 10923–32
51 Urbonite, S., and Novák, P., *Journal of Power Sources* 2014, **249**, 497-502
52 Diao, Y., Xie, K., Xiong, S., and Xiaobin, H. *Journal of the electrochemical society* 2012, **159(4)**, A421-A425
53 Fang, X., and Peng, H. *Small.* 2015, 11, **13**, 1488-1511
54 Lin, T., Tang, Y., Wang, Y., Bi, H., Liu, Z., Huang, F., Xie, X., and Jiang, M., *Energy Environ. Sci.* 2013, **6**, 1283-1290
55 Seh, Z. W., Li, W., Cha, J. J., Zheng, G., Yang, Y., McDowell, M. T., Hsu, P., and Cui, Y. *Nature Communications.* 2013, **4:1331**, 1-6
56 Wang, D., Zeng, Q., Zhou, G., Yin, L., Li, F., Cheng, H., Gentle, I. R., Lu, G. Q. M. *J.Mater. Chem. A.* 2013, **1**, 9382-9394
57 Jha, H., Buchberger, I., Cui, X., Meini, S., and Gasteiger, H. A. *Journal of the electrochemical society* 2015, **162(9)**, A1829-A1835
58 Scheers, J., Fantini, S., and Johansson, P., *Journal of Power Sources*, 2014, **255**, 204-218
59 Lin, Z., and Liang, C. *J. mater. Chem. A*, 2015, **3**, 936-958
60 Barghamadi, M., Best, A. S., Bhatt, A. I., Hollenkamp, A. F., Musameh, M., Rees, R. J. and Rüther, T. *Energy. Environ. Sci.* 2014, **7**, 3902-3920

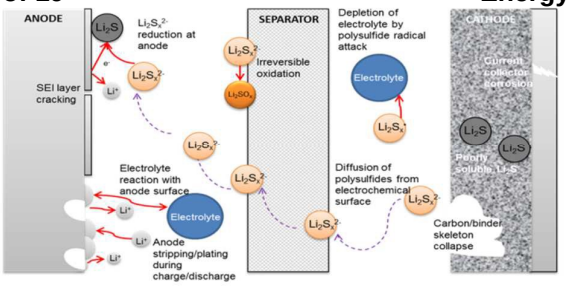

Lithium Sulfur Batteries, Review of current mechanistic understanding and the gap between experimentally derived mechanisms and those used for modelling